Marshall University
Marshall Digital Scholar

Physics Faculty Research | Physics

Fall 11-8-2010

Improved In Situ Spring Constant Calibration for Colloidal Probe Atomic Force Microscopy

Sean P. McBride
Marshall University, mcbrides@marshall.edu

Bruce M. Law

Follow this and additional works at: http://mds.marshall.edu/physics_faculty

 Part of the Physics Commons

Recommended Citation

McBride, S. P., & Law, B. M. (2010). Improved in situ spring constant calibration for colloidal probe atomic force microscopy. Review of Scientific Instruments, 81, 113703.

This Article is brought to you for free and open access by the Physics at Marshall Digital Scholar. It has been accepted for inclusion in Physics Faculty Research by an authorized administrator of Marshall Digital Scholar. For more information, please contact zhangj@marshall.edu, martj@marshall.edu.

AIP | Review of Scientific Instruments

Improved in situ spring constant calibration for colloidal probe atomic force microscopy

Sean P. McBride and Bruce M. Law

Citation: Review of Scientific Instruments **81**, 113703 (2010); doi: 10.1063/1.3502460
View online: http://dx.doi.org/10.1063/1.3502460
View Table of Contents: http://scitation.aip.org/content/aip/journal/rsi/81/11?ver=pdfcov
Published by the AIP Publishing

Articles you may be interested in

Accurate noncontact calibration of colloidal probe sensitivities in atomic force microscopy
Rev. Sci. Instrum. **80**, 065107 (2009); 10.1063/1.3152335

A calibration method for lateral forces for use with colloidal probe force microscopy cantilevers
Rev. Sci. Instrum. **79**, 023701 (2008); 10.1063/1.2836327

Calibration of colloid probe cantilevers using the dynamic viscous response of a confined liquid
Rev. Sci. Instrum. **74**, 4026 (2003); 10.1063/1.1597950

An improved wedge calibration method for lateral force in atomic force microscopy
Rev. Sci. Instrum. **74**, 3362 (2003); 10.1063/1.1584082

Calibration of the torsional spring constant and the lateral photodiode response of frictional force microscopes
Rev. Sci. Instrum. **71**, 2746 (2000); 10.1063/1.1150686

This article is copyrighted as indicated in the article. Reuse of AIP content is subject to the terms at: http://scitationnew.aip.org/termsconditions. Downloaded to IP: 128.135.100.108 On: Sun, 28 Dec 2014 19:34:21

Improved *in situ* spring constant calibration for colloidal probe atomic force microscopy

Sean P. McBride and Bruce M. Law
Department of Physics, Cardwell Hall, Kansas State University, Manhattan, Kansas 66506-2601, USA

(Received 30 July 2010; accepted 27 September 2010; published online 8 November 2010)

In colloidal probe atomic force microscopy (AFM) surface forces cannot be measured without an accurate determination of the cantilever spring constant. The effective spring constant k depends upon the cantilever geometry and therefore should be measured *in situ*; additionally, k may be coupled to other measurement parameters. For example, colloidal probe AFM is frequently used to measure the slip length b at solid/liquid boundaries by comparing the measured hydrodynamic force with Vinogradova slip theory (V-theory). However, in this measurement k and b are coupled, hence, b cannot be accurately determined without knowing k to high precision. In this paper, a new *in situ* spring constant calibration method based upon the residuals, namely, the difference between experimental force-distance data and V-theory is presented and contrasted with two other popular spring constant determination methods. In this residuals calibration method, V-theory is fitted to the experimental force-distance data for a range of systematically varied spring constants where the only adjustable parameter in V-theory is the slip length b. The optimal spring constant k is that value where the residuals are symmetrically displaced about zero for all colloidal probe separations. This residual spring constant calibration method is demonstrated by studying three different liquids (n-decanol, n-hexadecane, and n-octane) and two different silane coated colloidal probe-silicon wafer systems (n-hexadecyltrichlorosilane and n-dodecyltrichlorosilane). © *2010 American Institute of Physics.* [doi:10.1063/1.3502460]

I. INTRODUCTION

Since its first application by Ducker *et al.*[1,2] and Butt *et al.*[3] to measure colloidal, electrostatic, van der Waals, and hydration forces in electrolyte solutions, *colloidal probe* atomic force microscopy (AFM) has become an extremely popular technique for measuring forces. Colloidal probe AFM is capable of measuring small interaction forces, such as those associated with ion pairing,[4] molecular recognition of DNA-protein and enzyme-substrate reactions,[5] the Casimir effect,[6,7] adhesion,[8–11] and hydrodynamic drainage forces at solid-fluid interfaces.[12–26] Extensive reviews on AFM force measurements[27–29] highlight additional details and experiments performed with colloidal probe AFM.

In colloidal probe and noncolloidal probe AFM measurements,[30,31] assessing the spring constant k is the primary limiting factor in determining the accuracy of the force measurement. Early force experiments[1–3] relied on either using the often incorrect spring constants provided by the manufacturer, the parallel beam approximation for v-shaped cantilevers,[32,33] and/or spring constant equations containing only a single elastic modulus,[32,33] whereas most AFM cantilevers are composites of many different materials (e.g. base material, chromium, and gold) of differing thicknesses. Early work by Butt *et al.*[34] demonstrated a unique experimental method for determining k for v-shaped cantilevers which showed that k differed from the parallel beam approximation used for v-shaped cantilevers; this technique demonstrated that k for v-shaped noncolloidal cantilevers needed to be determined experimentally. Simultaneous independent efforts for v-shaped and beam cantilevers have lead to the popular Cleveland method,[35] thermal noise method,[36] and Sader methods.[37–40] Lévy and Maaloum[41] demonstrated excellent agreement between the thermal noise and Sader methods for noncolloidal rectangular cantilevers in air and highlighted some disagreements found in other noncolloidal v-shaped cantilever calibration methods.[42] Cook *et al.*[43] found that the thermal noise and Sader methods for noncolloidal rectangular cantilevers in air agreed to within ~4% over a wide range of cantilevers.

The cantilevers in most commercial AFMs are mounted at an angle,[43–45] and this tilt angle can result in an increase in the effective k by 10%–20%.[9,10] Edwards *et al.*[46] recently demonstrated that in addition to the tilt angle, the position of a *colloidal probe* placed at the end of the cantilever plays an important role in the inverse optical lever sensitivity[47] (InvOLS) and spring constant calibrations. In most AFMs the deflection of the cantilever is sensed by measuring the voltage sum signal reflected from the end of the cantilever on a position sensitive detector (PSD); this InvOLS process calibrates the PSD and encodes this voltage to deflection conversion (Appendix A). The work of Edwards *et al.* suggests that both the spring constant k and InvOLS calibrations should be conducted in the actual experimental configuration in order to correctly account for any tilts and induced torques associated with the colloidal probe. Craig and Neto[12] have developed a method that enables k to be calibrated *in situ* for colloidal probes; this method effectively accounts for these tilts and torques due to the placement of the colloidal probe. This method requires using a viscous liquid possessing a

 © 2010 American Institute of Physics

This article is copyrighted as indicated in the article. Reuse of AIP content is subject to the terms at: http://scitationnew.aip.org/termsconditions. Downloaded to IP: 128.135.100.108 On: Sun, 28 Dec 2014 19:34:21

zero slip length as a calibration fluid; however, it is often difficult to determine a priori if a particular liquid/solid combination possesses zero slip length. A very similar *in situ* calibration for colloidal probes was hypothesized earlier by Senden and Ducker.[48]

Following the work of Edwards *et al.*,[46] *in situ k* calibration of large colloidal probes for hydrodynamic force measurements implies that the probes must be immersed in viscous liquids where the viscosity can easily exceed that of water by a factor of 10 or greater. Current noncolloidal probe k calibration methods all have the same inherent problem when applied to colloidal probes conducted in this type of environment; they rely on the quality factor Q of the cantilever, which describes the sharpness of the resonant frequency peak of the cantilever, f_R. As has been previously shown even for noncolloidal probes, water drastically damps the oscillating cantilever, effectively lowering Q to the order of unity[49] and making the shape of the resonance peak less well defined.[50] For large colloidal probes in viscous liquids, the system is further damped ($Q \ll 1$) and the resonance peak becomes ill defined. Walters *et al.*[50] found that the thermal method in air and water for noncolloidal rectangular cantilevers agreed to within $\pm 11\%$ and $\pm 20\%$ for the Cleveland method. Later, Burnham *et al.*[45] compared the Cleveland, thermal noise, and Sader methods in both air and water environments for rectangular and v-shaped noncolloidal probes. Burnham *et al.* found the use of the Cleveland method inappropriate in a water environment, the Sader method determination of k ranged from 15%–40% lower in air than in water, and that the thermal method displayed differences as high as 60% depending upon the surrounding environment and shape of the cantilever.

In summary, different methods for determining the spring constant k of the AFM cantilever will depend upon the sample environment (e.g. air or liquid) and the cantilever geometry (e.g. rectangular versus v-shaped cantilevers, cantilever tilt, colloidal probe positioning). These factors can lead to differences in the spring constant k of up to 60%; thus, directly influencing how accurately a particular quantity can be measured using AFM. It is therefore clear that the spring constant k should be determined *in situ* in precisely the geometry that will be used for the actual AFM experiments. Any variations in the experimental geometry will require a recalibration of the spring constant k.

In this study, an experimental *in situ* calibration of the spring constant for large colloidal probes is demonstrated by adjusting k between experimental estimates until the residuals, exhibit minimal systematic deviation as a function of separation h. The residuals are defined as the difference between the experimental force-distance data and slip theory of Vinogradova[51] (V-theory). The experimental lower and upper estimates of k for the colloidal probes used in this study were determined by (i) the standard thermal noise method performed in air using the default InvOLS correction factor of $\chi = 1.09$,[50,52–54] (see Appendix B for details on this correction factor and improvements to the thermal noise method) and (ii) a method similar to the Craig and Neto *in situ* method[12] but conducted in a liquid of finite slip length. The residuals calibration is performed with decanol and two different silane coated surfaces to test reproducibility. Perfect agreement between experiment and V-theory would be indicated by the residuals being symmetrically displaced about zero as a function of separation. A plot of the residuals as a function of separation provides both a graphical and a numerical indicator (χ^2, the sum of the squares of the residuals) from which the correct k value representing the system can be determined. With this k value fixed, the slip length for any liquid can then be determined, provided that the cantilever geometry remains unaltered.

In an effort to remain focused on the residuals calibration method, the reader is referred to comprehensive review articles[55–58] that describe the many models, mechanisms, and measurements relating to slip and no-slip boundary conditions. This article is organized as follows. Characteristics of the surfaces used in the experiment are first given. This is followed by a brief description of the experimental setup and basic principles of colloidal probe atomic force microscopy. The foundation and results of the residuals spring constant calibration method are established in the main body of the paper. Important technical details, such as colloidal probe calibration, thermal noise method improvements, surface preparation, and cantilever drag analysis (required for a reader to reproduce the results) can be found in the appendices.

II. EXPERIMENTAL METHODS

V-shaped silicon nitride AFM cantilevers (NP-S series), with a quoted spring constant range of 0.06–0.58 N/m, were purchased from Veeco.[59] n-hexadecyltrichlorosilane (HTS) from Fluka and n-dodecyltrichlorosilane (DTS) from Gelest were used as received with no further purification. n-hexadecane (anhydrous, 99+%) and n-octane (98%) were purchased from Sigma Aldrich and used as received with no further purification. The silicon substrates with 1–10 Ω cm resistivity and $\langle 100 \rangle$ orientation were purchased from Silicon Materials Inc. The ~ 55 μm diameter borosilicate glass spheres, used as colloidal probes, were purchased from MO-SCI Specialty Products, L.L.C. All water used in this experiment was first purified by a custom reverse osmosis deionization system built by Siemens and then by a Millipore Academic A10 water purification system, which provided 18.2 MΩ cm resistivity at 25 °C. Unless otherwise specified, all other liquids in the experiment had a purity $\geq 99.5\%$ and were used as received from the respective manufacturers. All nitrogen drying, in the preparation steps as well as in experiments, was performed with ultrahigh purity dry nitrogen (99.999+%).

The attachment process of the colloidal probe to the AFM cantilever as well as the silanization process of both the colloidal probe and silicon wafer are described in Appendix C. Table I summarizes the surface characteristics of both the HTS and DTS silanized systems.

The root mean squared (rms) surface roughness value and peak-peak (p-p) asperity values are given on all surfaces; (5×5) and (2×2) μm^2 ac mode images were used to acquire rms measurements for the silane coated silicon substrates and colloidal probes, respectively. rms and asperities

This article is copyrighted as indicated in the article. Reuse of AIP content is subject to the terms at: http://scitationnew.aip.org/termsconditions. Downloaded to IP: 128.135.100.108 On: Sun, 28 Dec 2014 19:34:21

TABLE I. Silicon wafer and colloidal probe surface characteristics.

	rms (nm)	p-p max. (nm)	Area (μm^2)	Octane		Hexadecane		Decanol		H_2O	
				θ_{adv}	θ_{rec}	θ_{adv}	θ_{rec}	θ_{adv}	θ_{rec}	θ_{adv}	θ_{rec}
HTS silicon	0.22	3.2	5×5	12	10	40	37	45	40	110	104
DTS silicon	0.16	2.5	5×5	11	8	40	37	47	42	111	104
HTS probe	0.86	10.1	2×2	⋯	⋯	⋯	⋯	⋯	⋯	⋯	⋯
DTS probe	0.98	31.4	2×2	⋯	⋯	⋯	⋯	⋯	⋯	⋯	⋯

measurements for silicon substrates are averaged over three random spots on each silicon substrate. The rms measurement for the colloidal probes, at the point of contact (±0.5 μm), was determined by mounting the cantilever on a custom holder that compensated for the 11° cantilever holder tilt. Figure 1 shows an ac mode image of the HTS colloidal probe at the point of contact with the silicon substrate. Advancing and receding contact angle measurements (Table I) were made by increasing and decreasing the volume of water (octane, hexadecane, and decanol) on the silane coated silicon wafer using a Kent Scientific Genie Plus syringe pump. A long range microscope (First Ten Angstroms 100 Series) was used to record the images and determine the contact angles with an estimated accuracy of ±1°. Contact angle measurements were made by averaging three dynamic sessile drop experiments in similar droplet volume regimes. The difference between advancing and receding contact angles provides a measure of the chemical and physical homogeneity of the samples.[60] Contact angles on the colloidal probes were assumed to be similar to the flat silicon wafer values, however, they could be systematically lower by as much as ~10°.[61] Table I demonstrates that the HTS probe is far superior to the DTS probe, based upon the height of the asperities. The diameters of the colloidal probes used in the experiments were measured with estimated error of ~2% using a Lecia inverted optical microscope (DM IRM) with a 63× water immersion lens (resolution: 0.14 μm per pixel). For comparison, the local radius of curvature[62] of the colloidal probes was determined from the (2×2) μm^2 AFM scan and differed from the optical determination by less than 5% for both the DTS and HTS colloidal probes.

An atmospheric chamber has been integrated into the base of the Asylum Research MFP 3D AFM (three-dimensional molecular force probe) to minimize adsorption of any atmospheric contaminates/moisture onto the sample surfaces immediately prior to an experiment. The chamber has a built-in humidity sensor (La Crosse Technology model WS-7220U-IT) and temperature probe (Yellow Springs Instruments 44034 precision thermistor) which accurately measures the temperature to within ±0.1 °C (which is important because the liquid viscosities are sensitive to temperature[63]). Operation of the atmospheric chamber for each experiment is described in previous work.[24] Prior to purging the atmospheric chamber with nitrogen, both surfaces in all experiments are exposed to a 500 microcurie polonium 210 source (NRD L.L.C. Model 3C500) which effectively neutralizes any static charges. n-decanol (~11.2 mPa s at 25 °C) was chosen as the calibration liquid because it produces a large deflection of the cantilever. As described in detail in Appendix A, before each hydrodynamic force measurement, a slow approach at a drive velocity of 500 nm/s was performed in order to calibrate the InvOLS,[47] eliminate any *virtual deflection*,[21,23] and ensure that no residual charges were present on either surface. The combined 15 slow InvOLS approach runs prior to the fast runs for each colloidal probe showed very little deviation with average InvOLS values of (48.5±0.4) and (31.4±0.1) nm/V for HTS and DTS probes, respectively (each slow approach was performed on different spots on the silicon substrate). Unless otherwise specified, all hydrodynamic force measurements were performed in an open loop configuration at a drive velocity of ~40 μm/s with zero dwell time on the surface.

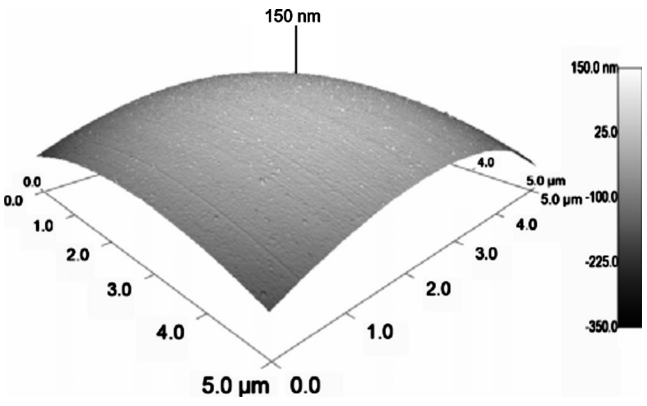

FIG. 1. ac mode image of the HTS colloidal probe at the point of contact.

As the colloidal probe approaches the silicon wafer surface during an experiment, the linear voltage displacement transducer (LVDT) of the AFM provides information about the piezoelectric displacement z of the base cantilever at each time interval. At each time interval the AFM also measures the total colloidal probe deflection x determined from the output voltage of the position sensitive detector (Appendix A). The separation h between the colloidal probe apex and the silicon substrate is given by the sum of the LVDT signal and deflection x ($h=z+x$). The velocity of the colloidal probe (dh/dt), which differs from the drive velocity of the cantilever (dz/dt),[64] is obtained by differentiating the probe separation h with respect to time.

III. ANALYSIS

A variety of forces contribute to the total force that acts on the colloidal probe; these forces include the hydrodynamic drag on the sphere (F_h), the hydrodynamic drag on the cantilever (F_{cant}), and surface forces between the sphere and substrate (F_{surf}), i.e. electrostatic interactions etc. For surface

This article is copyrighted as indicated in the article. Reuse of AIP content is subject to the terms at: http://scitationnew.aip.org/termsconditions. Downloaded to IP: 128.135.100.108 On: Sun, 28 Dec 2014 19:34:21

TABLE II. Summary of spring constants and slip lengths at ~40 μm/s cantilever velocity.

		$k_{thermal}$ Decanol	$k_{in\ situ}$ Decanol	$k_{residuals}$ Decanol	$k_{residuals}$ Hexadecane	$k_{residuals}$ Octane
HTS	k (N/m)	0.95 ± 0.08	1.38 ± 0.03	1.23 ± 0.01	1.23	1.23
	Slip (nm)	29.3 ± 1.7	11.7 ± 0.9	15.7 ± 1.1	20.4 ± 0.3	17.4 ± 0.5
DTS	k (N/m)	0.88 ± 0.10	1.31 ± 0.01	1.20 ± 0.01	1.20	1.20
	Slip (nm)	30.8 ± 0.7	11.4 ± 0.5	14.3 ± 0.5	14.3 ± 0.2	9.8 ± 1.8

separations $h \geq 10$ nm, provided that both the colloidal probe and the surface are uncharged, F_{surf} is negligible compared with F_h and will be neglected for the remainder of this discussion. The total experimental force on the colloidal probe is given as

$$F_e = kx = k(x_h + x_{cant}), \tag{1}$$

where x is the total cantilever deflection measured by the AFM. The deflection due to the hydrodynamic drag on the sphere (cantilever) is given by x_h (x_{cant}). The cantilever contribution, $F_{cant}=kx_{cant}$ which is included in Eq. (1) only makes a small constant contribution to the total force as determined experimentally in Appendix D ($F_{cant} \sim 1$ nN for decanol). The experimental hydrodynamic force due to the sphere, $F_e - F_{cant}$, can be compared with theory where

$$F_h = \frac{6\pi\eta r^2 v\psi}{h}. \tag{2}$$

η is the bulk viscosity, r is the radius of the sphere, h is the separation distance between the sphere and the solid surface, and $v=dh/dt$ is the approach/withdraw velocity of the sphere. From continuum hydrodynamics, Vinogradova[51] (V-theory) determined a relationship between ψ and the slip length b, which is valid for $h \ll r$, assuming the slip length b is independent of shear rate. For $b \neq 0$,

$$\psi = \frac{h}{3b}\left[\left(1+\frac{h}{6b}\right)\ln\left(1+\frac{6b}{h}\right)-1\right]. \tag{3}$$

As b approaches the no-slip boundary condition ($b \to 0$), the parameter $\psi \to 1$.

According to Eqs. (1) and (2), the residuals are defined as

$$R = kx_h - \frac{6\pi\eta r^2 v\psi}{h}, \tag{4}$$

which provides a measure of how well V-theory describes the experimental hydrodynamic force data. For perfect agreement between theory and experiment, the residuals R would be symmetrically displaced around zero when plotted as a function of separation h. Any systematic deviations of R from zero would imply that the two fitting parameters k and b that appear in Eqs. (3) and (4) are in error, or, the assumptions behind V-theory are incorrect. The residuals R therefore allow for a quantitative comparison of different spring constant determination methods.

A popular method for determining the spring constant of cantilevers is the thermal noise method.[36] This method is typically performed with noncolloidal cantilevers in air with the default InvOLS correction factor of $\chi=1.09$ (Refs. 50 and 52–54) (see Appendix B for details). This method allows for the determination of the spring constant k_{therm} by fitting the power spectrum of the cantilever thermal noise to a simple harmonic oscillator response with added white noise. It is a quick and simple process to determine k_{therm} using the default thermal noise model via the user interface provided with the Asylum Research 3D MFP AFM. If this value of $k=k_{therm}$ (calibrated in air) is used in Eq. (4) then the only free parameter with which to improve the agreement between experimental data and V-theory is the slip length b. Table II lists k_{therm} and the best fit values of the slip length b from six trials for the two different types of silane coatings (HTS and DTS) on the colloidal probe and Si wafer surface. Figure 2(a) (lower curve) shows a plot of the residuals R as a function of separation h for this thermal noise determination of the spring constant. R exhibits systematic deviations below zero, implying that the actual value for k representing our system is greater than k_{therm}. There are corrections to k_{therm} which account for the cantilever tilt and torque (Appendix B) however these corrections only marginally improve the residuals.

An alternative method for estimating the spring constant k is the *in situ* method developed by Craig and Neto.[12] This method assumes no-slip boundary conditions (i.e. $b=0$ nm

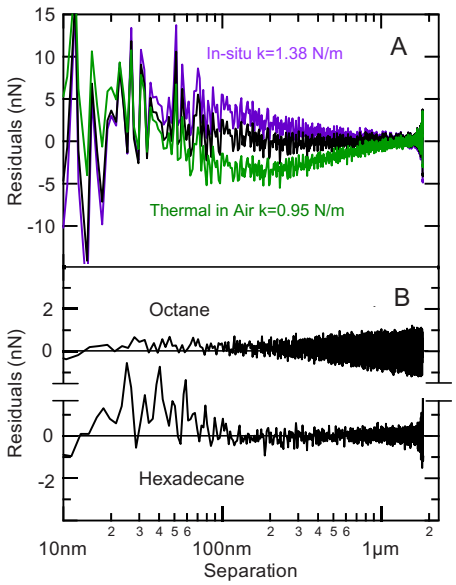

FIG. 2. (Color online) (a) Residuals from fitting V-theory to run five in decanol using the HTS system; *in situ* (upper line), residuals $k_{res}=1.23$ N/m (middle), and thermal (k calibrated in air) (lower). (b) Residuals for octane ($b=17.1$ nm) and hexadecane ($b=20.3$ nm) using fixed $k_{res}=1.23$ N/m for HTS system.

This article is copyrighted as indicated in the article. Reuse of AIP content is subject to the terms at: http://scitationnew.aip.org/termsconditions. Downloaded to IP: 128.135.100.108 On: Sun, 28 Dec 2014 19:34:21

and $\psi=1$) are valid at the solid-liquid interface. Therefore, according to Eqs. (1) and (2) if the viscosity and radius of the sphere are known, the "*in situ* spring constant," $k_{in\ situ}$, can be determined from the slope of a plot of the normalized deflection x_{norm} $(=x/v)$ versus the inverse separation h^{-1}

$$\frac{x}{v}=\frac{6\pi\eta r^2}{k_{in\ situ}}\left(\frac{1}{h}\right). \tag{5}$$

For our system, this $k_{in\ situ}$ method is only used as an approximation since it was originally intended to be performed in a liquid with no slip. As such, the protocol developed by Craig and Neto was followed with the exception that we only use the data far from the surface where the slip length contributes little to the reduction of the hydrodynamic force and the plot of x_{norm} versus h^{-1} remains linear. If this value of $k=k_{in\ situ}$ (conducted in decanol) is used in Eq. (4) then the only free parameter with which to improve the agreement between experimental data and V-theory is the slip length b. Table II lists $k_{in\ situ}$ and the best fit values of the slip length b from six trials for the two different types of silane coatings (HTS and DTS) on the colloidal probe and Si wafer surface. Figure 2(a) (upper curve) shows a plot of the residuals R as a function of separation h for this *in situ* determination of the spring constant. R exhibits systematic deviations above zero which implies that the actual value for k representing our system is less than $k_{in\ situ}$.

As is evident from Fig. 2(a) the actual spring constant representing our system must lie between k_{therm} and $k_{in\ situ}$. In the "residual method" for determining the optimal spring constant k_{res}, the chi-squared given by the sum of the squares of the residuals at each separation h, or

$$\chi^2=\sum_i [R_i(h)]^2 \tag{6}$$

is used. k_{res} will possess the lowest χ^2 where graphically R is distributed symmetrically about zero as a function of separation h. In practice, the spring constant is systematically adjusted between the experimental estimates k_{therm} and $k_{in\ situ}$ in 0.01 N/m increments. At each k value, the hydrodynamic drag from the cantilever is determined (Appendix D), the best fit slip length b is determined for all separations $h \geq 10$ nm, and χ^2 is calculated for separations $h \geq 100$ nm. This optimal k_{res} value is listed in Table II along with its best fit slip length; k_{res} possesses the lowest χ^2 value and exhibits minimal systematic deviations in the residuals as a function of separation [Fig. 2(a), horizontal curve]. The same deflection data used to determine $k_{in\ situ}$ in decanol are used to determine k_{res}. In order to confirm that k_{res} is the actual spring constant representative of our system, slip measurements for two other liquids, n-hexadecane and n-octane, were conducted with k_{res} fixed at 1.23 N/m (HTS system); these liquids possess viscosities of 3.0 and 0.5 mPa s at 25 °C, respectively, (whereas $\eta=11.2$ mPa s for n-decanol). In these experiments it is important that the geometry of the cantilever remain unchanged. For these liquids the only adjustable parameter is the slip length b; indeed the residuals are symmetrically displaced around zero for both liquids [Fig. 2(b)] which is further evidence that the residual method determines the actual cantilever spring constant.

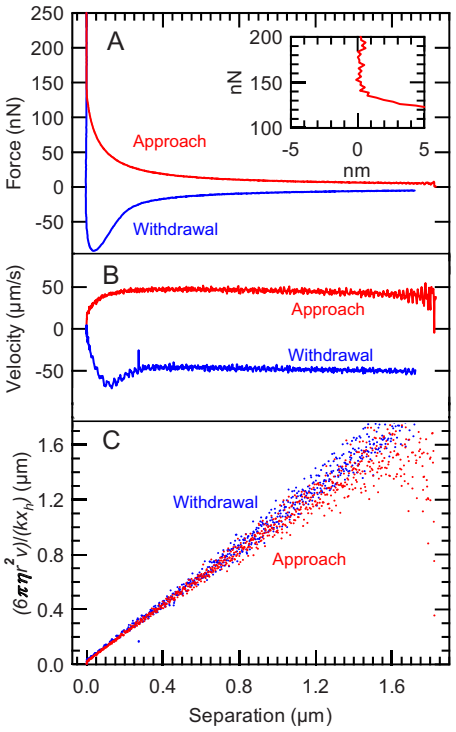

FIG. 3. (Color online) (a) Force, (b) velocity, and (c) expansion representation [Eq. (7)] for decanol run five HTS system. Inset A demonstrates that hard contact was made on approach at zero separation.

V-theory assumes that the slip length is constant and independent of the shear rate. This assumption is expected to be valid below a critical shear rate of $\dot{\gamma}_c \sim 10^{10}$ s^{-1} as determined from molecular dynamics simulations.[58] While our experimental shear rates $\dot{\gamma} \sim v/h < 10^4$ s^{-1} are well below $\dot{\gamma}_c$, nevertheless it is important to check this assumption experimentally. Multiple experiments were conducted at cantilever drive velocities of 10, 20, and 30 μm/s and no shear rate dependence of the slip length was observed in either the HTS or DTS systems. The average slip length b for n-decanol (with k_{res} fixed) was (16 ± 1) and (14 ± 1) nm for HTS and DTS, respectively (measurements averaged over 15 different runs).

Honig and Ducker[21–23] use an alternative method to verify the shear rate independence of the slip length. As demonstrated by Cottin-Bizonne *et al.*[65,66] Eqs. (1)–(3) can be expanded in the limit of large separations for $6b/h \ll 1$

$$\frac{6\pi\eta r^2 v}{kx_h}=h+2b. \tag{7}$$

A plot of the left hand side of Eq. (7) versus separation h, using $k=k_{\text{res}}$, should be linear (for large $h \gg 6b$) with a slope of 1 and a h-intercept at $h=-2b$, provided (i) the slip length is shear rate independent, (ii) the cantilever drag is correctly determined, and (iii) the radius and viscosity are accurately known. Figure 3 shows an analysis of n-decanol run five for the HTS system using this approach. Figure 3(a) shows the approach/withdrawal force data where the inset (for approach) demonstrates that hard contact was made between the sphere and the surface at zero separation. The approach/withdrawal velocities [Fig. 3(b)], calculated from Fig. 3(a) $(v=dh/dt)$, are quite different and are not constant. Despite

This article is copyrighted as indicated in the article. Reuse of AIP content is subject to the terms at: http://scitationnew.aip.org/termsconditions. Downloaded to IP: 128.135.100.108 On: Sun, 28 Dec 2014 19:34:21

this large variation in velocity, a plot based upon Eq. (7) is linear for both approach and withdrawal where both data sets collapse onto a single line with no oscillations as shown in Fig. 3(c). By fitting the separation data in Fig. 3(c) between 200 nm and 1 μm for the HTS system, slopes of 0.99 and 1.04 were obtained for approach and withdrawal (similar slopes were obtained for the DTS system). All of the slopes are very close to unity; the approach data are in slightly better agreement with Eq. (7) than the withdrawal data, most likely due to the fact that only the approach InvOLS was used to calibrate the system. The slip length can also be extracted from Eq. (7) by extrapolating the approach data, in the separation range from 200 nm to 1 μm, to the h-intercept. For run five of the HTS decanol system (run 1 of the DTS decanol system) a slip length of 19.0 nm (16.0 nm) was obtained, which is in close agreement with the residual method results in Table II. Our preference is to use the residual method to determine the slip length, which avoids extrapolations over large distances associated with Eq. (7).

IV. SUMMARY AND DISCUSSION

This publication presents a new *in situ* colloidal probe spring constant k calibration method that is applicable to all users of colloidal probe AFM. This new technique is based upon examining the residuals Eq. (4). The residuals used specifically in this study are the differences between experimental colloidal probe force-distance data and Vinogradova slip theory. The k value is adjusted between k_{therm} and $k_{in\ situ}$ in 0.01 N/m increments and V-theory is fitted to the force-distance data where the only adjustable parameter in V-theory is the slip length b. The optimal k value is where the residuals are symmetrically displaced about zero for all separations h. The calibration allows for an *in situ* determination of the AFM cantilever spring constant that is representative of the system. The residual spring constant calibration for n-decanol k_{res} indeed exhibits minimal deviations symmetrically displaced about zero as a function of separation as shown in Fig. 2(a) (middle line).

In order to determine the most accurate value for k using this residual calibration method, very large borosilicate spheres of diameter $2r \sim 55$ μm attached to v-shaped cantilevers were used. n-decanol was chosen as the calibration liquid as it possesses a large viscosity, $\eta \sim 11.2$ mPa s at 25 °C. The combination of large r and η provides a large hydrodynamic force F_h [Eq. (2)] for our colloidal probes, hence, making our measurements very sensitive to the precise value of k. Use of such large colloidal probes possesses other advantages: (i) the cantilever drag force (Appendix D) is relatively small and (ii) large separations ($h \sim 2$ μm) can be used while still remaining in the regime where $h \ll r$, as required by V-theory. Additional constraints, important in this work, are that the silicon wafer surface and colloidal probe possess low rms surface roughness and few, if any, large asperities. The n-alkyl silane coating (Appendix C) is of high quality, as demonstrated by the low contact angle hysteresis given in Table I.

This residuals spring constant method is reproducible to within 1% over six runs for each of the two silane coated systems that were examined (Table II). The expansion representation[65,66] [Eq. (7), Fig. 3(c)] and varying cantilever drive velocity tests all indicate that the slip length b is shear rate independent as assumed in V-theory. To check that k_{res} is indeed the actual cantilever spring constant for our system, the residuals of two other liquids (n-hexadecane and n-octane) were examined where k_{res} is fixed and the only adjustable parameter is the slip length b. The residuals for both of these liquids exhibit no systematic deviations as a function of separation [Fig. 2(b)]. In these experiments it is important that the geometry of the cantilever remains unchanged in order that the tilt contribution to the cantilever spring constant remains unaltered.

Two other popular spring constant calibration methods have also been evaluated using the residuals in this publication. The thermal noise spring constant k_{therm}, without the additional corrections described in Appendix B, is approximately 25% below the value determined via the residual calibration method which results in a slip length which is overestimated by a factor of 2 (Table II). The residuals from this thermal method consistently deviate below zero [Fig. 2(a), lower curve]. Although there are corrections to the thermal noise method which can account for the tilt and torque (Appendix B), these corrections are insufficient to account for the difference between k_{therm} and k_{res}. The *in situ* method of Craig and Neto provides a more reliable estimate of the spring constant compared with the thermal noise method because it intrinsically includes contributions from the tilt and torque due to the geometry of the cantilever and attached colloidal probe. However, this latter method assumes that the slip length is zero at the solid-liquid interface. For the n-decanol calibration liquid that was examined, the *in situ* method overestimates the cantilever spring constant $k_{in\ situ}$ relative to the residual calibration method by approximately 10%; consequently, the residuals for the *in situ* method consistently deviate above zero [Fig. 2(a), upper curve]. This overestimate for the spring constant leads to a lower slip length, relative to the residuals calibration method, by approximately 20%–25% (Table II).

The residuals spring constant calibration method developed in this study can be applied to any colloidal probe configuration with any cantilever shape as long as the total drag force of the colloidal probe and cantilever is known. This calibration method will be of immediate interest to spherical colloidal probe users in hydrodynamic drainage experiments where the drag force on the spherical probe has been well established.[51,67] Apart from accurately knowing the sphere radius and liquid viscosity, the only additional stipulations for using this residuals calibration are that the colloidal probe and surface are sufficiently smooth and the system must be immersed in a viscous Newtonian fluid.

Finally, we note that use of the residuals is quite general. They can be used to determine the spring constant in the presence of other surface forces F_{surf} provided that an accurate theoretical functional form for these other surface forces is known. If both the hydrodynamic force F_h as well as F_{surf} are present then these two contributions to the total force should be separable provide that F_h and F_{surf} exhibit differing functional forms as a function of the separation h.

This article is copyrighted as indicated in the article. Reuse of AIP content is subject to the terms at: http://scitationnew.aip.org/termsconditions. Downloaded to IP: 128.135.100.108 On: Sun, 28 Dec 2014 19:34:21

ACKNOWLEDGMENTS

S.P.M. would like to thank Dr. C. D. F. Honig for useful discussions. The authors would also like to extend their thanks and gratitude to the support staff at Asylum Research for technical discussions regarding the MFP 3D AFM and associated software and also thank numerous delegates at the inaugural Faraday Discussion Graduate Research Seminar and 146th Faraday Discussion meeting for useful comments and feedback. This research was conducted with the support from the National Science Foundation under Grant No. DMR-0603144.

APPENDIX A: COLLOIDAL PROBE CALIBRATION

In order to make it easier to replicate this work a number of technical issues are discussed in these appendices. In the Asylum Research MFP-3D AFM, the cantilever is attached to a LVDT which provides the z position of the cantilever. A laser beam reflects off the end of the cantilever onto a PSD. The PSD signal, once calibrated, provides information about the deflection x of the cantilever. Following standard practice, this distance to voltage calibration or InvOLS is deduced from the region of constant compliance where the colloidal probe is in hard contact with the silicon wafer.[47] With the liquid of interest in thermal equilibrium, the AFM head is leveled, and the InvOLS calibration is performed using a slow drive velocity of 500 nm/s where the colloidal probe is pushed against the Si wafer substrate. During the InvOLS calibration, when in the constant compliance region, the rate of change of the cantilever deflection is equal to the rate of change of the LVDT signal. Thus, the known LVDT signal is used to calibrate the PSD output voltage. Ideally, if the cantilever behaves as a simple spring, the PSD voltage will increase linearly with the LVDT signal. If nonlinearities in the constant compliance region are present they are most likely due to some nonlinear mechanical behavior of the cantilever as the properties of the PSD have less than a 0.5% nonlinearity throughout the full range of the PSD.[68] The InvOLS calibration and all hydrodynamic measurements are conducted only in the linear constant compliance region between ~0 and 5 V on the PSD. In practice, a slow (500 nm/s) InvOLS calibration is completed before each individual fast (~40 μm/s) hydrodynamic force measurement; corrections are also made to remove any *virtual deflection*.[21,23] The separation between the colloidal probe and the silicon surface, required in the analysis, is given by $h=x+z$. During a fast hydrodynamic force measurement, the zero of separation (when the surfaces are in hard contact) is determined by the presence of a vertical force when plotted as a function of separation [Fig. 3(a) inset]. The presence of a vertical force can only be obtained if and only if hard contact between the sphere and Si substrate is made and the InvOLS calibration is valid at the point of contact. The zeros of approach and withdrawal are chosen for each individual run based upon this vertical force, thus avoiding the hysteresis inherent in the LVDT signal, as described in similar experiments.[21,23,44]

Sader[69] suggests the universal use of beam shaped AFM cantilevers based upon theoretical calculations that illustrate that v-shaped cantilevers are more susceptible to lateral forces. For the v-shaped colloidal probe cantilevers used in this study, the relevant parameters that determine the (noncontact) lateral forces are the ratios of the colloidal probe position to the cantilever length, $\Delta L/L$ (=0.14) and the cantilever width to v-cross section, d/b (=0.25). Figure 4 in Sader[69] implies that beam shaped cantilevers with these dimensions will be only marginally more stable to lateral forces compared with v-shaped cantilevers of the same spring constant. In this work, v-shaped cantilevers were used because of our extensive experience at successfully attaching colloidal spheres centered and directly behind the pyramidal imaging tip (Appendix C). The v-shaped cantilevers also allow for reproducible placement of the maximized sum signal, which occurs in only one location.

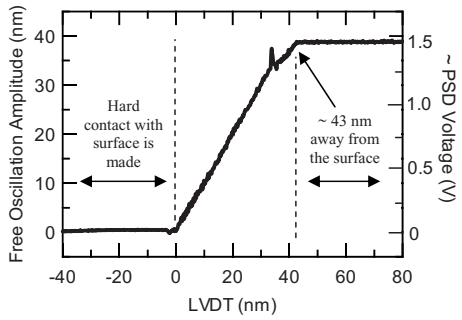

FIG. 4. Free oscillation amplitude/PSD voltage signal in air as a function of the LVDT signal for a noncolloidal NP-S series probe from Veeco.

APPENDIX B: IMPROVEMENTS TO THE THERMAL NOISE CALIBRATION

In Sec. III k_{therm} calibrated in air was used as a lower estimate of the colloidal probe spring constant. For convenience the default settings on the Asylum Research MFP 3D AFM were used in evaluating k_{therm} of the assembled colloidal probes. In reality, there are several corrections that could be applied to provide a better estimate of the *effective* thermal noise spring constant.

k_{therm} is determined by fitting the power spectrum of the colloidal probe thermal noise to a simple harmonic oscillator (SHO) response with added white noise; the adjustable parameters of the SHO fit are W_N the white noise, A the amplitude at dc,[70] f the resonant frequency, and Q the quality factor of the resonant frequency peak of the cantilever. The fit values of A, f, and Q are then used in the default thermal spring constant model in the Asylum Research MFP 3D

$$k_{\text{therm}} = \frac{2k_BT}{\pi A^2 f Q}, \tag{B1}$$

where k_B is Boltzmann's constant, T is the temperature (preprogrammed to be a constant at 16.6 °C). In the thermal noise method, the end of the cantilever is free to oscillate at its natural resonant frequency far from the surface. In this situation the $\text{InvOLS}_{\text{free}}$ value describes how the cantilever bends when freely oscillating. The InvOLS determined from the region of constant compliance used to calibrate the PSD is only applicable for an end loaded cantilever ($\text{InvOLS}_{\text{end}}$) where the cantilever is not allowed to oscillate. Despite recent efforts to determine $\text{InvOLS}_{\text{free}}$,[71] typically $\text{InvOLS}_{\text{free}}$ is

This article is copyrighted as indicated in the article. Reuse of AIP content is subject to the terms at: http://scitationnew.aip.org/termsconditions. Downloaded to IP: 128.135.100.108 On: Sun, 28 Dec 2014 19:34:21

calculated from $\mathrm{InvOLS}_{\mathrm{end}}$ by assuming a default correction factor[50,52–54] $\chi=\mathrm{InvOLS}_{\mathrm{free}}/\mathrm{InvOLS}_{\mathrm{end}}=1.09$. This default InvOLS correction factor is expected to depend upon the focused laser spot size and position on the cantilever.[53] V-shaped cantilevers are expected to have different thermal fluctuation responses when compared to beam shaped cantilevers;[29,72] these differences in thermal fluctuations due to cantilever shape can be taken into account by experimentally determining the $\mathrm{InvOLS}_{\mathrm{free}}$ value.

$\mathrm{InvOLS}_{\mathrm{free}}$ can be determined experimentally using an ac force approach.[73] Figure 4 for a noncolloidal v-shaped cantilever shows the damping of the free amplitude oscillation as the surface is approached. $\mathrm{InvOLS}_{\mathrm{free}}$ is calibrated from the linear variation in PSD signal as a function of LVDT signal immediately before hard contact. For this specific v-shaped cantilever the average InvOLS correction factor is $\chi=1.07\pm0.04$ (which is close to the default value derived for beam shaped cantilevers, despite the fact that we are using a v-shaped cantilever). Difficulties arise in determining $\mathrm{InvOLS}_{\mathrm{free}}$ when the large 55 μm diameter colloidal probe is attached to the AFM cantilever. The accuracy of the thermal method for use with these large colloidal probes could be improved by being able to experimentally determining the $\mathrm{InvOLS}_{\mathrm{free}}$ value and not relying on the default correction value of $\chi=1.09$. For both colloidal and noncolloidal probes having a nonfixed temperature would also improve the accuracy of the default thermal model. Note that $\mathrm{InvOLS}_{\mathrm{free}}$ ($\mathrm{InvOLS}_{\mathrm{end}}$) is called Amp InvOLS (Def InvOLS) in the Asylum Research MFP 3D AFM software.

The tilt of the cantilever and attachment of the colloidal probe can markedly change the effective cantilever spring constant k_{eff} compared with the intrinsic cantilever spring constant k_z.[46] More specifically, in the notation used by Edwards *et al.*[46]

$$k_{\mathrm{eff}}=k_z\left(\frac{T_z}{\cos^2\theta}\right), \tag{B2}$$

where the term in parenthesis is the correction to the spring constant due to cantilever tilt $\theta=11°$ and colloidal probe attachment with "torque correction" T_z. From the measured dimensions of our v-shaped silicon nitride cantilever with attached silica colloidal probe[69,74] $k_{\mathrm{eff}}=1.08$ N/m (1.00 N/m) for the HTS (DTS) probe assuming that $k_{\mathrm{therm}}=k_z$. Although k_{eff} is 14% larger than k_{therm} these corrections still do not fully account for the ~25% difference between k_{therm} and k_{res}.

APPENDIX C: SILICON WAFER AND COLLOIDAL PROBE PREPARATION

In order to produce n-alkyl silane coated Si wafers possessing low contact angle hysteresis (Table I), the following procedure was followed: (i) new Si wafers were sonicated in acetone, (ii) plasma cleaned (Harrick PDC-3G) followed by CO_2 snow-jet cleaning at ~300 °C, (iii) step (ii) was repeated, (iv) sonication in ethanol, and then (v) a final sonication in toluene. After each sonication step the Si wafer was dried with N_2 gas. The Si wafers were then immediately piranha cleaned for 2 h (equal volumes of 97.3% concentrated H_2SO_4 and 31.5% concentrated H_2O_2), rinsed well in 90–100 °C Millipore water, and then quickly dried with a heat gun. A wet chemical silanization technique[75] was modified and used as a guide for the silanization process. The Si samples were immediately transferred to room temperature toluene (50 ml). The Si/toluene temperature was then lowered to 0 °C (10 °C) if the silanization involved DTS (HTS) in a dry box (relative humidity < 12%) and allowed to reach thermal equilibrium over the course of 1 h. The desired silane (0.02 ml) was added with the syringe tip submerged under the cold toluene liquid-vapor interface to avoid silane polymerization. The solution was stirred and left undisturbed for 5 h. Upon removal, the Si wafers were rinsed twice with fresh chloroform, and then CO_2 snow-jet cleaned prior to any measurements.

To prepare similarly well-coated colloidal probes having low surface roughness and few asperities, the following protocol was devised: the MO-SCI silica spheres were first etched in a continuously stirred basic solution of $C_2H_6O:KOH:H_2O$ in a ratio 50 ml: 6 g: 6 ml for 2 h, repeatedly rinsed in continuously stirred 90–100 °C Millipore water, followed by two continuously stirred fresh ethanol rinses The spheres were then carefully dried with a heat gun. A clean microscope slide was then coated with a vapor deposited trichloro(3,3,3-trifluoro-propyl)silane layer. The excess silane was wiped off with chloroform and a lens cloth and then CO_2 snow-jet cleaned. A light dusting of the dried spheres was spread over the glass microscope slide and mounted on the *x-y* scanner of the AFM. AC mode AFM imaging was used to identify useable spheres of low surface roughness with few asperities. The useable spheres were attached to the desired AFM cantilevers (Veeco NP-S 0.58 N/m nominal spring constants) using the AFM head as follows. Excess cantilevers were first removed from the cantilever chip. The desired cantilever was then precleaned by rinsing in chloroform and carbon tetrachloride and then exposed to short wave UV ozone. A small amount of UV curable epoxy (Norland 61) was placed at the end of the cantilever using a separate optical microscope setup. The NP-S cantilever with UV glue then replaces the standard imaging tip in the AFM head. With the position of the *x-y* scanner remaining unchanged, the colloidal sphere possessing low surface roughness and few asperities remains directly under the NP-S cantilever. Using the three leveling legs of the AFM and the two *x-y* adjustment knobs for the *x-y* scanner, the colloidal sphere was precisely attached, centered immediately behind the pyramidal tip of the AFM cantilever as the AFM head is lowered. Once the sphere is attached to the cantilever, the apex is then reimaged to characterize the rms, it is then exposed to long wave UV for 2 h to set the glue, and then heated at 50 °C for 12 h to fully cure the glue. Once cured, Norland 61 is highly chemically resistant to many organic solvents. The colloidal probes were then plasma cleaned, decharged with a 500 microcurie polonium-210 source, and then silane coated as described above. Upon removal from the silane, chloroform rinses were used to remove excess silane.

In studying different liquids using the same colloidal probe and Si wafer, the AFM colloidal probe holder and Si

This article is copyrighted as indicated in the article. Reuse of AIP content is subject to the terms at: http://scitationnew.aip.org/termsconditions. Downloaded to IP: 128.135.100.108 On: Sun, 28 Dec 2014 19:34:21

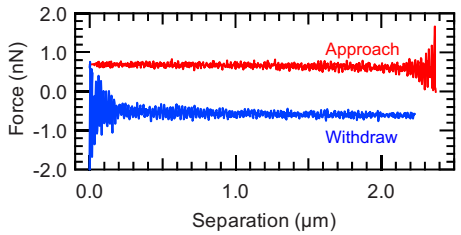

FIG. 5. (Color online) Cantilever drag force F_{cant} in decanol determined for a noncolloidal NP-S series probe at a height of ~55.0–57.5 μm from the surface.

wafer were rinsed well and/or sonicated in chloroform, blown dry, and then vacuum dried before the next experiment. The cantilever chip was left in the cantilever holder during all the above cleaning steps and the AFM leveling legs were not coarsely adjusted between experiments, thus keeping the geometry of the colloidal probe the same when studying different liquids.

APPENDIX D: CANTILEVER DRAG F_{cant}

In colloidal probe AFM, a number of different groups[21,25,76] have attempted to model the cantilever drag F_{cant} in order to subtract this contribution from the total experimental force, thus just leaving the colloidal probe contribution F_h. The drag force on the cantilever is not very easy to model accurately; therefore, F_{cant} has been experimentally measured for a noncolloidal cantilever similar to the ones used in this study. For the large colloidal probes of diameter ~55 μm, F_{cant} is expected to be a small constant force which is independent of the separation h. F_{cant} was measured in n-decanol at ~40 μm/s over a distance of 2 μm at a height of ~55 μm above the surface using a *noncolloidal* Veeco NP-S series cantilever with a measured spring constant k_{therm}=0.40 N/m. The noncolloidal cantilever k has been determined using the thermal noise calibration method in air where $InvOLS_{free}$ calibration was experimentally determined using an ac force approach (Appendix B).

F_{cant} has been accounted for as follows. The total experimental force is given by $F_e=F_h+F_{cant}$ where F_{cant} is a constant as shown by Fig. 5, while F_h is well represented by the Brenner[67] no-slip result (or equivalently V-theory with $b \rightarrow 0$) at least at large separations where slip effects are negligible. For each run, F_{cant} is determined at large separations ($h \sim 1.5–2$ μm) by finding the difference between F_e and V-theory with b=0.1 nm; this difference is then subtracted from F_e. F_{cant} ranged from 0.9 to 1.2 nN for HTS and DTS, in close agreement with the results in Fig. 5.

[1] W. A. Ducker, T. J. Senden, and R. M. Pashley, Nature (London) **353**, 239 (1991).
[2] W. A. Ducker, T. J. Senden, and R. M. Pashley, Langmuir **8**, 1831 (1992).
[3] H.-J. Butt, Biophys. J. **60**, 1438 (1991).
[4] E. Spruijt, M. A. Cohen Stuart, and J. van der Gucht, Macromolecules **43**, 1543 (2010).
[5] K. Kurihara, in *Nanohybridization of Organic-Inorganic Materials*, edited by A. Muramatsu and T. Miyashita (Springer, Berlin, 2009), Vol. 13, pp. 125–137.
[6] U. Mohideen and A. Roy, Phys. Rev. Lett. **81**, 4549 (1998).
[7] G. L. Klimchitskaya, U. Mohideen, and V. M. Mostepanenko, Rev. Mod. Phys. **81**, 1827 (2009).
[8] M. Kappl and H.-J. Butt, Part. Part. Syst. Charact. **19**, 129 (2002).
[9] L.-O. Heim, M. Kappl, and H.-J. Butt, Langmuir **20**, 2760 (2004).
[10] J. L. Hutter, Langmuir **21**, 2630 (2005).
[11] S. Leporatti, R. Sczech, H. Riegler, S. Bruzzano, J. Storsberg, F. Loth, W. Jaeger, A. Laschewsky, S. Eichhorn, and E. Donath, J. Colloid Interface Sci. **281**, 101 (2005).
[12] V. S. J. Craig and C. Neto, Langmuir **17**, 6018 (2001).
[13] V. S. J. Craig, C. Neto, and D. R. M. Wiliams, Phys. Rev. Lett. **87**, 054504 (2001).
[14] E. Bonaccurso, M. Kappl, and H.-J. Butt, Phys. Rev. Lett. **88**, 076103 (2002).
[15] G. Sun, E. Bonaccurso, V. Franz, and H.-J. Butt, J. Chem. Phys. **117**, 10311 (2002).
[16] E. Bonaccurso, H.-J. Butt, and V. S. J. Craig, Phys. Rev. Lett. **90**, 144501 (2003).
[17] C. Neto, V. S. J. Craig, and D. R. M. Williams, Eur. Phys. J. E **12**, 71 (2003).
[18] O. I. Vinogradova and G. E. Yakubov, Langmuir **19**, 1227 (2003).
[19] J.-H. J. Cho, B. M. Law, and F. Rieutord, Phys. Rev. Lett. **92**, 166102 (2004).
[20] O. I. Vinogradova and G. E. Yakubov, Phys. Rev. E **73**, 045302 (2006).
[21] C. D. F. Honig and W. A. Ducker, J. Phys. Chem. C **111**, 16300 (2007).
[22] C. D. F. Honig and W. A. Ducker, Phys. Rev. Lett. **98**, 028305 (2007).
[23] C. D. F. Honig and W. A. Ducker, J. Phys. Chem. C **112**, 17324 (2008).
[24] S. P. McBride and B. M. Law, Phys. Rev. E **80**, 060601(R) (2009).
[25] S. Guriyanova, B. Semin, T. S. Rodriques, H.-J. Butt, and E. Bonaccurso, Microfluid. Nanofluid. **8**, 653 (2010).
[26] T. S. Rodrigues, H.-J. Butt, and E. Bonaccurso, Colloids Surf., A **354**, 72 (2010).
[27] H.-J. Butt, M. Jaschke, and W. A. Ducker, Bioelectrochem. Bioenerg. **38**, 191 (1995).
[28] B. Cappella and G. Dietler, Surf. Sci. Rep. **34**, 1 (1999).
[29] H.-J. Butt, B. Cappella, and M. Kappl, Surf. Sci. Rep. **59**, 1 (2005).
[30] G. Binnig, C. F. Quate, and C. Gerber, Phys. Rev. Lett. **56**, 930 (1986).
[31] G. Binnig, C. Gerber, E. Stoll, T. R. Albrecht, and C. F. Quate, Europhys. Lett. **3**, 1281 (1987).
[32] T. R. Albrecht, S. Akamine, T. E. Carver, and C. F. Quate, J. Vac. Sci. Technol. A **8**, 3386 (1990).
[33] D. Sarid and V. Elings, J. Vac. Sci. Technol. B **9**, 431 (1991).
[34] H.-J. Butt, P. Siedle, K. Sefert, K. Fendler, T. Seeger, E. Bamberg, L. Weisenhorn, K. Goldie, and A. Engel, J. Microsc. **169**, 75 (1993).
[35] J. P. Cleveland, S. Manne, D. Bocek, and P. K. Hansma, Rev. Sci. Instrum. **64**, 403 (1993).
[36] J. L. Hutter and J. Bechhoefer, Rev. Sci. Instrum. **64**, 1868 (1993).
[37] J. E. Sader and L. White, J. Appl. Phys. **74**, 1 (1993).
[38] J. E. Sader, P. Mulvaney, I. Larson, and L. R. White, Rev. Sci. Instrum. **66**, 3789 (1995).
[39] J. E. Sader, J. Appl. Phys. **84**, 64 (1998).
[40] J. E. Sader, J. W. M. Chon, and P. Mulvaney, Rev. Sci. Instrum. **70**, 3967 (1999).
[41] R. Lévy and M. Maaloum, Nanotechnology **13**, 33 (2002).
[42] J. M. Neumeister and W. A. Ducker, Rev. Sci. Instrum. **65**, 2527 (1994).
[43] S. M. Cook, T. E. Schäffer, K. M. Chynoweth, M. Wigton, R. W. Simmonds, and K. M. Lang, Nanotechnology **17**, 2135 (2006).
[44] P. Attard, A. Carambassis, and M. W. Rutland, Langmuir **15**, 553 (1999).
[45] N. A. Burnham, X. Chen, C. S. Hodges, G. A. Matei, E. J. Thoreson, C. J. Roberts, M. C. Davies, and S. J. B. Tendler, Nanotechnology **14**, 1 (2003).
[46] S. A. Edwards, W. A. Ducker, and J. E. Sader, J. Appl. Phys. **103**, 064513 (2008).
[47] G. Meyer and N. M. Amer, Appl. Phys. Lett. **53**, 1045 (1988).
[48] T. J. Senden and W. A. Ducker, Langmuir **10**, 1003 (1994).
[49] M. B. Viani, T. E. Schäffer, A. Chand, M. Rief, H. E. Gaub, and P. K. Hansma, J. Appl. Phys. **86**, 2258 (1999).
[50] D. A. Walters, J. P. Cleveland, N. H. Thomson, and P. K. Hansma, Rev. Sci. Instrum. **67**, 3583 (1996).
[51] O. I. Vinogradova, Langmuir **11**, 2213 (1995).
[52] H.-J. Butt and M. Jaschke, Nanotechnology **6**, 1 (1995).
[53] R. Proksch, T. E. Scäffer, J. P. Cleveland, R. C. Callahan, and M. B. Viani, Nanotechnology **15**, 1344 (2004).
[54] T. E. Schäffer, Nanotechnology **16**, 664 (2005).
[55] O. I. Vinogradova, Int. J. Min. Process. **56**, 31 (1999).
[56] J. S. Ellis and M. Thompson, Phys. Chem. Chem. Phys. **6**, 4928 (2004).
[57] C. Neto, D. R. Evans, E. Bonaccurso, H.-J. Butt, and V. S. J. Craig, Rep. Prog. Phys. **68**, 2859 (2005).

This article is copyrighted as indicated in the article. Reuse of AIP content is subject to the terms at: http://scitationnew.aip.org/termsconditions. Downloaded to IP: 128.135.100.108 On: Sun, 28 Dec 2014 19:34:21

[58] E. Lauga, M. P. Brenner, and H. A. Stone, *Handbook of Experimental Fluid Dynamics* (Springer, New York, 2007).
[59] Colloidal probes were glued to pre-December-2008 NP-S series AFM cantilevers that were distributed by Veeco. These probes originally had a Pyrex base to which the silicon nitride cantilevers were bonded to. Unfortunately, the manufacturing process has changed and it is no longer possible to glue colloidal probes to the more recent NP-S cantilevers produced by Veeco Probes. The newer cantilevers bend during the glue curing process.
[60] L. Gao and T. J. McCarthy, Langmuir **22**, 6234 (2006).
[61] M. Preuss and H.-J. Butt, J. Colloid Interface Sci. **208**, 468 (1998).
[62] C. Neto and V. S. J. Craig, Langmuir **17**, 2097 (2001).
[63] C. L. Yaws, *Handbook of Viscosity* (Gulf, Houston, TX, 1995), Vols. I–III.
[64] B. Semin, S. Guriyanova, and E. Bonaccurso, Rev. Sci. Instrum. **77**, 116107 (2006).
[65] C. Cottin-Bizonne, B. Cross, A. Steinberger, and E. Charlaix, Phys. Rev. Lett. **94**, 056102 (2005).
[66] C. Cottin-Bizonne, A. Steinberger, B. Cross, O. Raccurt, and E. Charlaix, Langmuir **24**, 1165 (2008).
[67] H. Brenner, Chem. Eng. Sci. **16**, 242 (1961).
[68] Every MFP 3D AFM is currently checked by the test department to have less than a 0.5% nonlinearity throughout the full range of the PSD. In most cases less than 0.2% throughout the full PSD range is achieved.
[69] J. E. Sader, Rev. Sci. Instrum. **74**, 2438 (2003).
[70] The zero frequency amplitude, or amplitude at dc, is equivalent to the thermal dc value in the Asylum Research Software.
[71] M. J. Higgins, R. Proksch, J. E. Sader, M. Polick, S. McEndoo, J. P. Cleveland, and S. P. Jarvis, Rev. Sci. Instrum. **77**, 013701 (2006).
[72] R. W. Stark, T. Drobek, and W. M. Heckl, Ultramicroscopy **86**, 207 (2001).
[73] P. Fontaine, P. Guenoun, and J. Daillant, Rev. Sci. Instrum. **68**, 4145 (1997).
[74] Cantilever tilt 11°, colloidal probe angle 5.5°, H=56 μm, cantilever leg width d=31 μm, V cross-section b=122 μm, length L=114 μm, colloidal probe attachment point relative to cantilever tip 16 μm, and silicon nitride Poisson's ratio 0.24.
[75] J. B. Brzoska, I. Ben Azouz, and F. Rondelez, Langmuir **10**, 4367 (1994).
[76] O. I. Vinogradova, H.-J. Butt, G. E. Yakubov, and F. Feuillebois, Rev. Sci. Instrum. **72**, 2330 (2001).

This article is copyrighted as indicated in the article. Reuse of AIP content is subject to the terms at: http://scitationnew.aip.org/termsconditions. Downloaded to IP: 128.135.100.108 On: Sun, 28 Dec 2014 19:34:21